Kinetics of Histidine Deligation from the Heme in GuHCl-Unfolded Fe(III) Cytochrome *c* Studied by a Laser-Induced pH-Jump Technique

Stefania Abbruzzetti,[†] Cristiano Viappiani,*[,†] Jeanne R. Small,[‡] Louis J. Libertini,[§] and Enoch W. Small[§]

Contribution from the Dipartimento di Fisica, Università di Parma, Istituto Nazionale per la Fisica della Materia, 43100 Parma, Italy, Department of Chemistry and Biochemistry, Eastern Washington University, Cheney, Washington 99004, and Quantum Northwest, Inc., Spokane, Washington 99224

Received January 8, 2001. Revised Manuscript Received April 20, 2001

Abstract: We have developed an instrumental setup that uses transient absorption to monitor protein folding/unfolding processes following a laser-induced, ultrafast release of protons from *o*-nitrobenzaldehyde. The resulting increase in $[H^+]$, which can be more than 100 μM, is complete within a few nanoseconds. The increase in $[H^+]$ lowers the pH of the solution from neutrality to approximately 4 at the highest laser pulse energy used. Protein structural rearrangements can be followed by transient absorption, with kinetic monitoring over a broad time range (∼10 ns to 500 ms). Using this pH-jump/transient absorption technique, we have examined the dissociation kinetics of non-native axial heme ligands (either histidine His26 or His33) in GuHCl-unfolded Fe(III) cytochrome *c* (cyt *c*). Deligation of the non-native ligands following the acidic pH-jump occurs as a biexponential process with different pre-exponential factors. The pre-exponential factors markedly depend on the extent of the pH-jump, as expected from differences in the pK_a values of His26 and His33. The two lifetimes were found to depend on temperature but were not functions of either the magnitude of the pH-jump or the pre-pulse pH of the solution. The activation energies of the deligation processes support the suggestion that GuHCl-unfolded cyt *c* structures with non-native histidine axial ligands represent kinetic traps in unfolding.

Introduction

The folding and unfolding kinetics of cytochrome *c* (cyt *c*) have been the subject of several studies using various methodologies,[1−4] including ultrafast pulsed-laser-based techniques.[5] In the native protein, the heme iron is coordinated to two axial ligands—an imidazole nitrogen from His18 and a thioether sulfur from Met80.[6] In increasing concentrations of GuHCl, Fe(III) cyt *c* undergoes a cooperative transition with a midpoint of 2.7 M GuHCl at neutral pH.[7] In addition to peptide conformational changes,[7] the transition involves replacement of the Met80 axial ligand by a histidine residue, and both His26 and His33 have been implicated as ligands in the GuHCl-unfolded cyt *c* (cyt c_{Gu}). Recent work suggests that His33 dominates.[8,9] Thus, cyt c_{Gu} may be viewed as comprised of two subpopulations, one with His26 occupying the axial site vacated by Met80 (cyt c_{Gu}-His26), and the other with His33 occupying that axial site. The non-native histidine−iron ligation in cyt c_{Gu} at pH 7 introduces a kinetic barrier for folding that allows the trapping of a nativelike intermediate with interacting N- and C-terminal helices.[10,11] Under acidic conditions, at least one of the non-native axial ligands (His26 and His33) has been found to be replaced by water.[1,9] The native histidine ligand, His18, is strongly bound to the heme (pK_a = 2.8 for Fe(III) cyt *c*)[8] by virtue of its position on the polypeptide chain—next to Cys17, which forms a thioether linkage with the porphyrin.

The Soret absorbance band of cyt *c* is very sensitive to ligation and spin state.[12,13] Cyt c_{Gu} has a Soret absorbance maximum at 407 nm. When the pH of a cyt c_{Gu} solution is lowered, the Soret absorbance band shifts to a maximum of ∼400 nm. This finding is consistent with loss of a strong-field ligand, coupled with protonation of a side-chain nitrogen. Kinetic investigations (stopped-flow pH-jump monitored by absorbance) of Fe(III)−histidine deligation in cyt c_{Gu} have shown biphasic behavior with well-separated rates in the millisecond range at room temperature. The two transients have been attributed to deligation of the non-native histidines in the two populations, cyt c_{Gu}−His26 and cyt c_{Gu}−His33, with replacement by a water molecule.[1,9]

* To whom correspondence should be addressed. Tel.: +390521905208. Fax: +390521905223. E-mail: cristiano.viappiani@fis.unipr.it.
[†] Università di Parma.
[‡] Eastern Washington University.
[§] Quantum Northwest, Inc.

(1) Colon, W.; Elöve, G. A.; Wakem, L. P.; Sherman, F.; Roder, H. *Biochemistry* **1996**, *35*, 5538−5549.
(2) Bixler, J.; Bakker, G.; McLendon, G. *J. Am. Chem. Soc.* **1992**, *114*, 6938−6939.
(3) Yeh, S. R.; Rousseau, D. L. *Nat. Struct. Biol.* **1998**, *5*, 222−227.
(4) Pierce, M. M.; Nall, B. T. *Protein Sci.* **1997**, *6*, 618−627.
(5) Jones, C. M.; Henry, E. R.; Hu, Y.; Chan, C.; Luck, S. D.; Bhuyan, A.; Roder, H.; Hofrichter, J.; Eaton, W. A. *Proc. Natl. Acad. Sci. U.S.A.* **1993**, *90*, 11860−11864.
(6) Bushnell, G. W.; Louie, G. V.; Brayer, G. D. *J. Mol. Biol.* **1990**, *214*, 585−595.
(7) Hamada, D.; Kuroda, Y.; Katoaka, M.; Aimoto, S.; Yoshimura, T.; Goto, Y. *J. Mol. Biol.* **1996**, *256*, 172−186.
(8) Telford, J. R.; Tezcan, F. A.; Gray, H. B.; Winkler, J. R. *Biochemistry* **1999**, *38*, 1944−1949.
(9) Colon, W.; Wakem, L. P.; Sherman, F.; Roder, H. *Biochemistry* **1997**, *36*, 12535−12541.
(10) Roder, H.; Elöve, G. A.; Englander, S. W. *Nature* **1988**, *335*, 700−704.
(11) Elöve, G. A.; Bhuyan, A. K.; Roder, H. *Biochemistry* **1994**, *33*, 6925−6935.
(12) Ikai, A.; Fish, W. W.; Tanford, C. *J. Mol. Biol.* **1973**, *73*, 165−184.
(13) Brems, D. N.; Stellwagen, E. *J. Biol. Chem.* **1983**, *258*, 3655−3660.

10.1021/ja010079n CCC: $20.00
Published on Web 06/14/2001

In the present work, we have used a laser pH-jump methodology with transient absorption detection to study the kinetics of nonnative axial ligand substitution upon acidification of Fe(III) cyt *c* unfolded in 3.1 and 4.5 M GuHCl. These two concentrations have been selected to have a direct comparison with available literature data.[8,9] We have employed *o*-nitrobenzaldehyde (*o*-NBA) as a photoactivatable caged proton and a nanosecond ultraviolet laser to generate the ultrafast acidification. The present approach allows us to perform kinetic investigations extending from nanoseconds to hundreds of milliseconds, thereby expanding the characterization of ligand substitution kinetics into the submillisecond time scale. We have recently applied the nanosecond pH-jump methodology with photoacoustic detection to study volume changes accompanying the acid-induced formation of a molten globule state in apomyoglobin[15] and the acid-induced formation or destruction of local helical structure in model polypeptides.[16,17] This paper reports the first application of the nanosecond pH-jump methodology to study protein folding events by means of transient absorption.

Experimental Methods

Materials. Horse heart Fe(III), cyt *c*, *o*-NBA, and GuHCl were obtained from Sigma-Aldrich.

Solutions were freshly prepared before use and saturated with nitrogen to remove dissolved CO_2. The pre-pulse pH was adjusted to the desired value by addition of concentrated NaOH or HCl. Experiments were conducted in either 3.1 or 4.5 M GuHCl aqueous solutions in the absence of buffer salts. Absorption spectra were measured with a computer-interfaced spectrophotometer (Jasco 7850).

The absorbance of *o*-NBA at the excitation wavelength (355 nm) was kept at $\sim$2 cm^{-1} in all of the experiments.

Laser-Flash Photolysis Setup. The laser pH-jump apparatus was a substantial modification of a previously described setup.[18] The third harmonic (355 nm, 160 mJ) of a nanosecond, Q-switched Nd:YAG laser (Surelite II-10, Continuum) was used to photolyze *o*-NBA and induce the release of protons to the solution containing horse heart Fe(III) cyt *c*. The beam was passed through a variable attenuator (Eksma) and focused to a horizontal line with a 0.5-m cylindrical lens. The monitoring beam was either a multiline, single-mode, cw argon-ion laser (JDS Uniphase, 150 mW all lines: 458, 476, 488, 497, and 514 nm) or a HeNe laser (NEC Corp., 10 mW, 633 nm). The desired output line from the argon laser was separated using a prism (Pellin Broca) and an iris diaphragm. The beam was passed through a rectangular quartz cuvette (4 mm $\times$ 10 mm) along the 10-mm path, at a right angle to the pump beam, and as close as possible to the face of the cuvette receiving the pump beam. The cuvette was held in a temperature-controlled sample holder (FLASH 100, Quantum Northwest, Inc.) and flushed with nitrogen to prevent condensation at low temperatures and to minimize CO_2 uptake by the solutions during the kinetic experiments. The transmitted intensity of the cw beam was monitored by a large-area, avalanche silicon photodiode (Hamamatsu, S2385), and the output voltage was amplified using two cascaded broadband operational amplifiers (Burr Brown, OPA643, gain 49$\times$). The overall bandwidth was about 200 MHz. A 0.25-m monochromator (H25, Jobin Yvon) was placed before the photodiode in order to remove stray light from the pump laser. The voltage signal was digitized by a digital sampling oscilloscope (LeCroy 9370, 1GHz, 1GS/s).

The sample was changed after each flash. To increase the signal-to-noise ratio, the pulse traces from four to nine samples were averaged.

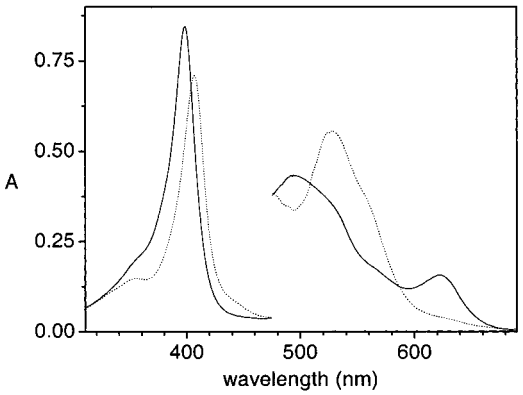

Figure 1. Absorption spectra of a 6.5 μM cyt *c* solution in 4.5 M GuHCl at pH 6.5 (dotted line) and pH 4 (solid line). The data for $\lambda >$ 475 nm are shown on a $\times$10 expanded absorbance scale.

Data Analysis. Nonlinear least-squares fitting to sums of exponentials was performed with Origin 6.0 (Microcal) for single-curve analysis. For all the transients, double-exponential decay functions showed much better fits than single, and little or no improvement was obtained with three exponentials. Global analysis (simultaneous analysis of several decay curves) was performed with a dedicated Matlab program (The Mathworks) using an optimization package (Minuit) with results that were also consistent with a double-exponential decay model. In the experiments varying either pre-pulse pH or laser pulse energy (at constant temperature), the global analysis was conducted with the lifetimes (τ_i) as shared parameters. In the temperature-dependence experiments, global analysis was performed with the lifetimes constrained either through the Arrhenius (eq 1) or the Eyring (eq 2) relations:[19]

$$\ln(k_i) = \ln(k_i^0) - \frac{E_a}{RT} \tag{1}$$

$$\ln\left(\frac{hk_i}{kT}\right) = \frac{\Delta S^{\ddagger}}{R} - \frac{\Delta H^{\ddagger}}{RT} \tag{2}$$

In these equations $k_i = 1/\tau_i$ is the rate constant of process *i* ($i = 1$ or 2), *h* is Planck's constant, *k* is the Boltzmann constant, *R* is the gas constant, and *T* is the temperature (K). When using eq 1 the activation energy (E_a) and k_i^0 were the shared parameters; with eq 2 they were the activation entropy and enthalpy ($\Delta S^{\ddagger}$ and $\Delta H^{\ddagger}$).

Results and Discussion

Figure 1 shows the absorption spectra of cyt c_{Gu} at pH 6.5 and 4.0. When the pH of the solution is lowered, the absorption spectrum shifts to the blue, indicating that the heme is being converted from a low-spin state (consistent with two axial histidine ligands at pH 6.5) to a mixed-spin or high-spin state (as a consequence of the loss of the non-native axial histidine ligand at pH 4.0).[20] Fitting of the pH dependence of the absorbance at 633 nm with the equation

$$A = A_0 + A_1 \frac{10^{n(\mathrm{pH} - \mathrm{p}K_a)}}{1 + 10^{n(\mathrm{pH} - \mathrm{p}K_a)}} \tag{3}$$

yielded p$K_a = 5.3 \pm 0.1$ and $n = 1.3 \pm 0.2$, consistent with the previously reported values.[8,9,14] The same behavior with pH was found when the experiment was repeated at 3.1 M GuHCl.

When *o*-NBA is photolyzed at pH > 3.5, protons are released to the solution within a few nanoseconds with a quantum yield of 0.4.[17,21,22] The deprotonation reaction can be followed by

(14) Tsong, T. Y. *Biochemistry* **1975**, *14*, 1542−1547.
(15) Abbruzzetti, S.; Crema, E.; Masino, L.; Vecli, A.; Viappiani, C.; Small, J. R.; Libertini, L. J.; Small, E. W. *Biophys. J.* **2000**, *78*, 405−415.
(16) Abbruzzetti, S.; Viappiani, C.; Small, J. R.; Libertini, L. J.; Small, E. W. *Biophys. J.* **2000**, *79*, 2714−2721.
(17) Viappiani, C.; Abbruzzetti, S.; Small, J. R.; Libertini, L. J.; Small, E. W. *Biophys. Chem.* **1998**, *73*, 13−22.
(18) Viappiani, C.; Bonetti, G.; Carcelli, M.; Ferrari, F.; Sternieri, A. *Rev. Sci. Instrum.* **1998**, *69*, 270−276.
(19) Laidler, K. J. *Chemical Kinetics*; HarperCollins: New York, 1987.
(20) Babul, J.; Stellwagen, E. *Biochemistry* **1972**, *11*, 1195−1200.
(21) George, M. V.; Scaiano, J. C. *J. Phys. Chem.* **1980**, *84*, 492−495.

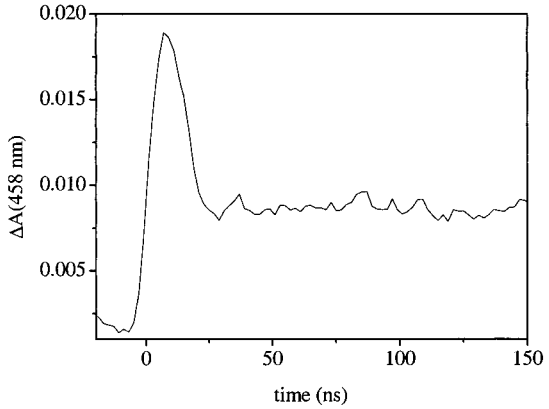

Figure 2. Transient absorption at 458 nm following photoexcitation of a neutral aqueous solution of *o*-NBA by a laser pulse at 355 nm. The trace is the average of nine single shots. Transient absorption at 633 nm showed no signal following photolysis at 355 nm.

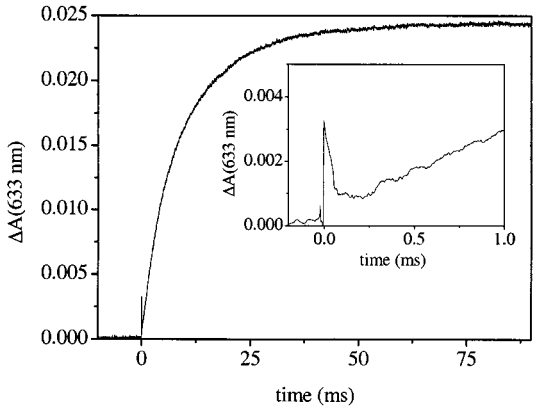

Figure 3. Transient absorption at 633 nm following a nanosecond acidification of 6.5 μM cyt *c* in 4.5 M GuHCl. The samples included *o*-NBA to give an absorbance at 355 nm of 2 cm^{-1}. The trace is the average of four separate samples, $E_{355} = 56$ mJ, pre-pulse pH 7.38, 20 °C. Inset: The first millisecond of the signal with expanded scales.

monitoring either the transient absorption of the *aci*-nitro intermediate in the blue-violet region,[21,23] or the structural volume changes accompanying the reaction.[17,22,24]

Figure 2 shows a typical transient absorption trace, measured at 458 nm, after photolysis (355-nm laser pulse) of a neutral aqueous solution containing only *o*-NBA. The fast rise in absorbance corresponds to the formation of the *aci*-nitro intermediate, which is known to occur on a subnanosecond time scale.[25−27] The rate of disappearance of the *aci*-nitro intermediate, corresponding to the fast decay of the absorbance, is at the very limit of the experimental resolution for our setup. Fitting of the experimental trace in Figure 2 gave a lifetime of about 6 ns for the decay of the *aci*-nitro intermediate. The plateau region of Figure 2, from 50 ns onward, is assigned to the absorbance of the photoproduct, *o*-nitrosobenzoic acid, with an absorption spectrum showing a band in the blue region. The *o*-nitrosobenzoic acid is a strong acid and completely dissociates above pH 3.5. No long-lived intermediate is detectable with transient absorbance. In the red region of the spectrum, where analysis of cyt c_{Gu} is performed, no transients are evident. Photoacoustic experiments showed that this photoinduced reaction is accompanied by a contraction of the solution (between −5 and −9 mL/mol in neutral aqueous solutions, depending on the presence of other solutes) that occurs within the experimental time resolution (∼20 ns).[22,24]

When *o*-NBA is photoexcited in the presence of acceptors (in our experiments cyt c_{Gu}), the rapid acidification perturbs the equilibria between the solutes toward the protonated forms. In our case, the reaction of interest is protonation of His26 and His33 in the two cyt c_{Gu} subpopulations, which leads to deligation of the non-native residues from heme Fe(III).

Figure 3 shows the transient absorbance, measured at 633 nm, after photolysis of a neutral aqueous solution containing *o*-NBA in the presence of cyt c_{Gu} at room temperature. The change in absorbance is well fit by a double-exponential decay with lifetimes (relative amplitudes) of 4.4 ± 0.1 (42%) and 13.6 ± 0.1 ms (58%). A combination of pH-jump stopped-flow experiments with site-directed mutagenesis has been used to identify two transients arising from detachment of His26 and His33 from the cyt c_{Gu} iron.[9] On the basis of the similarities between those results and the decay results obtained here, we attribute our two transients to the kinetics of the two individual subpopulations, cyt c_{Gu}−His26 (4.4 ms) and cyt c_{Gu}−His33 (13.6 ms).

The absorption change in Figure 3 has a sign and magnitude consistent with the changes expected when the pH is lowered below neutrality, as is evident from Figure 1. In particular, a spectral band centered at 620 nm, which is absent for the cyt c_{Gu} at pH 6.5, is formed upon acidification of the solution. No signal is observed at 633 nm for a control solution containing *o*-NBA in the absence of cyt *c*. When cyt c_{Gu} alone is examined, a transient absorbance is observed at all of the monitoring wavelengths used, with the weakest signal observed at 633 nm. However, these signals are completely extinguished within 0.1 ms, and we suggest that they may be derived from the formation of a heme triplet state. No significant, long-lasting alterations in the absorbance spectrum of cyt c_{Gu} alone at any wavelength are observed after exposure to the intense 355-nm flash. The contribution of this microsecond cyt c_{Gu} transient to the signal measured in the presence of *o*-NBA is evident in the inset of Figure 3, where the first millisecond of data appears after the flash is shown. It is clear that this transient can only marginally affect the slower signal arising from pH-induced deligation, and the data can be corrected by subtraction of an appropriately scaled "background" transient. After subtraction, the signal extrapolates back to 0 at $t = 0$ s.

Experiments conducted on solutions containing cyt c_{Gu} and *o*-NBA using the argon-ion laser lines (458, 476, 488, 497, and 514 nm) gave results that were indistinguishable (within the uncertainty of the measurements) from those obtained with the HeNe laser at 633 nm. A comparison between signals measured under the same experimental conditions at 458 and 633 nm is shown in Figure 4. However, at the wavelengths available with the argon-ion laser, the transient absorption from the heme triplet is much larger than at 633 nm, and the resulting signals are more difficult to analyze, especially in the submillisecond range. This feature is evident as a positive spike in the short time scale of the 458-nm trace in Figure 4. A contribution to this spike also derives from photolysis of *o*-NBA at this wavelength (see discussion of Figure 2). In addition, a step increase in absorbance due to the photolysis of *o*-NBA is observed at 458 nm and

(22) Pelagatti, P.; Carcelli, M.; Viappiani, C. *Isr. J. Chem.* **1998**, *38*, 213−221.
(23) McCray, J. A.; Trentham, D. R. *Annu. Rev. Biophys. Biophys. Chem.* **1989**, *18*, 239−270.
(24) Bonetti, G.; Vecli, A.; Viappiani, C. *Chem. Phys. Lett.* **1997**, *269*, 268−273.
(25) Yip, R. W.; Sharma, D. K.; Giasson, R.; Gravel, D. *J. Phys. Chem.* **1984**, *88*, 5770−5772.
(26) Yip, R. W.; Sharma, D. K.; Giasson, R.; Gravel, D. *J. Phys. Chem.* **1985**, *89*, 5328−5330.
(27) Yip, R. W.; Wen, Y. X.; Gravel, D.; Giasson, R.; Sharma, D. K. *J. Phys. Chem.* **1991**, *95*, 6078−6081.

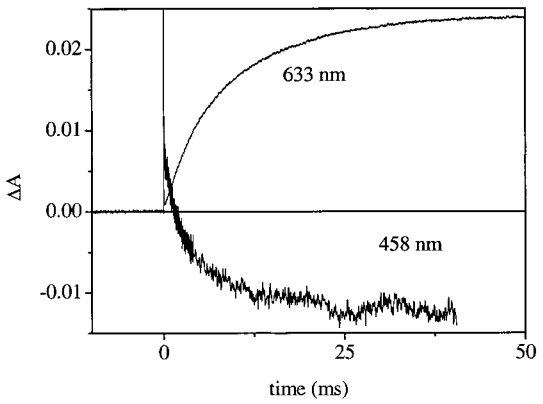

Figure 4. Comparison between the transient absorbance signals measured at 458 and 633 nm at 20 °C, pre-pulse pH 7.38, and E_{355} = 60 mJ. The solutions contained *o*-NBA (A_{355} = 2 cm^{-1}), Fe(III) cyt *c* (10 μM), and GuHCl (3.1 M).

results in a positive offset of the measured transient absorbance trace (Figure 4).

The different noise level between the two traces in Figure 4 is due to the lower signal measured at 458 nm, deriving from a combination of lower laser power and reduced photodiode sensitivity. Figure 4 and analyses of those traces suggest that the millisecond kinetics associated with the non-native His deligation are substantially the same at both wavelengths. However, because of the much lower signal-to-noise ratio for the results at lower wavelengths, all further results and discussion will be limited to the data obtained using the HeNe laser line, which was used to monitor the transient absorption at 633 nm.

Other neutralization reactions will be occurring on the protein, primarily binding of protons by carboxylate. Such reactions are unlikely to directly affect the absorbance of cyt c_{Gu}. Neutralization of carboxylates may contribute indirectly to His deligation; however, it is much more likely that perturbation of the equilibria between ligated His, free His, and protonated His by the added protons is primarily responsible for the absorbance changes illustrated in Figure 1. Binding of protons by the His residues is a fast process. A recent detailed kinetic analysis of proton binding by the protonatable sites on tuna cyt *c*[28] showed that His26 (which, in the native protein, is solvent exposed) binds protons with a bimolecular binding rate of 5×10^9 M^{-1} s^{-1}, a value consistent with other rates reported in the literature.[15,29,30] In our case, due to the disordered structure of cyt c_{Gu}, it is difficult to foresee the presence of proton transfer from nearby carboxylates to either His26 or His33,[28] but it seems reasonable to assume that the effect would be an increase in the observed binding rate.[30] Using the literature value for the bimolecular binding rate, under our experimental conditions ([cyt *c*] $\approx$ 10 μM) the apparent binding rate of protons to free His should be on the order of 10^5 s^{-1} or larger (decay time less than $\sim$10 μs). Besides, no specific change in absorbance should be associated with this proton-binding step. Dissociation of the non-native His from the heme (in response to the much lower concentration of unprotonated His) is a process occurring at a much slower rate, as evidenced by the kinetics results in Figures 3 and 4.

When the magnitude of the laser-induced pH-jump (increase in [H$^+$]) was varied by changing the energy of the 355-nm pulse, a biexponential decay function was obtained in every case. Separate analyses of the resulting decays gave lifetimes that

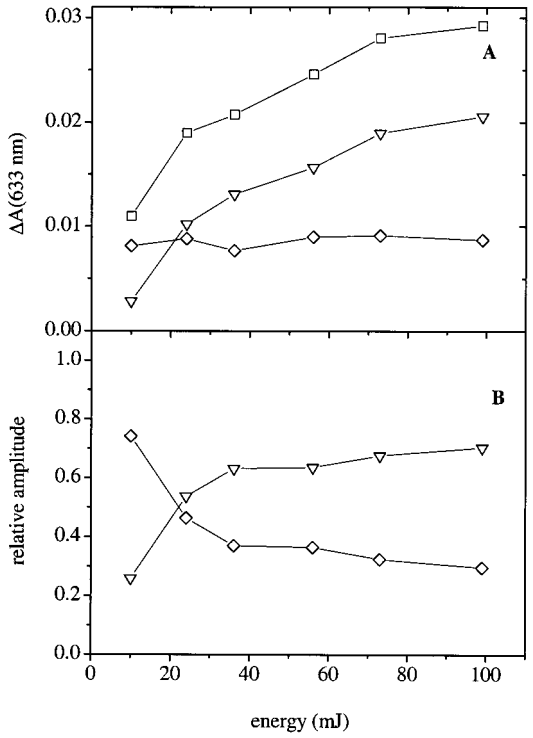

Figure 5. Results of global analysis of data obtained with increasing 355-nm pulse energy (increasing magnitude of the pH jump). (A) Absorbance changes of the fast (3.7 $\pm$ 0.1 ms, diamonds) and slow (13.1 $\pm$ 0.1 ms, triangles) decays and total change in absorbance (sum of the pre-exponentials, squares) at 633 nm as a function of laser pulse energy. Experiments were conducted at 20 °C and included *o*-NBA (A_{355} = 2 cm^{-1}), Fe(III) cyt *c* (10 μM), and GuHCl (4.5 M). (B) Relative amplitudes of the two decays.

were relatively independent of the increase of [H$^+$], indicating that these slow kinetics represent unimolecular reactions (i.e., having insignificant contributions from the kinetics of binding of [H$^+$]). Figure 5 shows the results of a global analysis of the transient absorbance traces, collected at 25 °C, in which lifetimes were shared parameters and no restrictions were placed on the amplitudes. The lifetimes obtained were 3.7 $\pm$ 0.1 and 13.1 $\pm$ 0.1 ms. Figure 5A shows the energy dependence of the absolute amplitudes of the two exponentials and the total absorbance change. The amplitude of the fast component (3.7 ms) is constant, whereas the amplitude of the slower decay (13.1 ms) increases with the laser pulse energy. At the laser pulse energy of 100 mJ, the total change in absorbance is identical with the change observed at equilibrium when the pH is lowered from 7 to 4. This indicates that a single, 100-mJ laser pulse can decrease the pH from neutrality to $\sim$4. Taking into account the fact that part of the photodetached protons are buffered by carboxylates on the protein, the actual concentration of protons released by the laser pulse would be >100 μM.

Our results imply that deligation of His26 is complete, even at the lowest increase in proton concentration (i.e., the lowest 355-nm pulse energy). This finding is consistent with results obtained for an H33N mutant (lacking His33), for which a transition pK_a of 6.11 was found from equilibrium data.[9] In contrast, we observed saturation for the amplitude of the slower decay only at laser pulse energies of $\geq$100 mJ. Further increasing the laser pulse energy above 100 mJ did not lead to significant changes. The H26Q mutant (lacking His26) has a transition pK_a of 5.6,[9] confirming that the pK_a for the overall transition of the wild-type protein is mainly determined by His33. This lower pK_a of His33 requires a larger pH-jump to achieve deligation of all His33.

(28) Marantz, Y.; Nachliel, E. *Isr. J. Chem.* **1999**, *39*, 439−445.
(29) Gutman, M.; Nachliel, E. *Biochim. Biophys. Acta* **1990**, *1015*, 391−414.
(30) Gutman, M.; Nachliel, E. *Annu. Rev. Phys. Chem.* **1997**, *48*, 329−356.

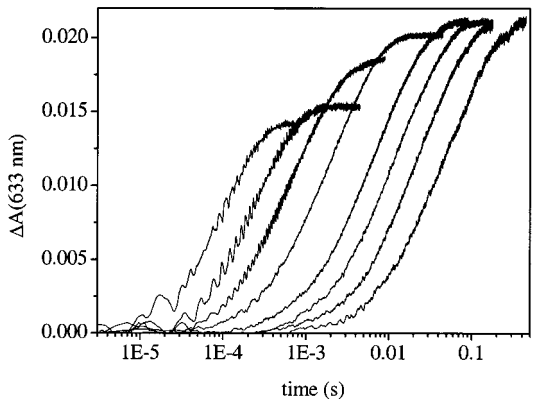

Figure 6. Transient absorbance traces measured at 633 nm after photolysis of solutions containing *o*-NBA ($A_{355} = 2$ cm^{-1}), Fe(III) cyt *c* (10 μM), and GuHCl (4.5 M) with the pre-pulse pH 7.38 at different temperatures. The temperatures corresponding to the various curves are, from left to right: 60, 50, 40, 30, 20, 15, 10, and 5 °C.

Table 1. Activation Parameters[a] for the Deligation Kinetics Determined by Global Analysis of the Transient Absorption Traces[b]

	E_a (kcal mol^{-1})	k^0 (s^{-1})	$\Delta S^{\ddagger}$ (cal K^{-1} mol^{-1})	$\Delta H^{\ddagger}$ (kcal mol^{-1})
His33	22.2 ± 0.6	$2.9 \times \mathbf{10}^{18}$	24 ± 2	21.6 ± 0.5
His26	18.4 ± 0.7	$1.6 \times \mathbf{10}^{16}$	13 ± 2	17.8 ± 0.7

[a] Values were determined using 3.1 and 4.5 M GuHCl; only values for 4.5 M GuHCl are reported here. [b] Traces were conducted at several temperatures.

Figure 5B shows that the relative amplitudes of the two transients reach saturating values of ~30% (3.7 ms) and 70% (13.1 ms) at high laser pulse energy, in good accordance with stopped-flow experiments.[9]

As for the steady-state results, no differences were seen in the cyt c_{Gu}−His26 and cyt c_{Gu}−His33 kinetics when the GuHCl concentration was lowered from 4.5−3.1 M.

When we performed experiments as a function of the pre-pulse pH value, at constant laser pulse energy, the amplitudes of the pre-exponentials resulting from global analysis showed a sigmoidal pH dependence (data not shown). This is in agreement with the equilibrium data. No signal was observable at pre-pulse pH below 4, as expected for complete deligation of the non-native histidines.

The temperature dependence of the deligation kinetics was measured in order to estimate the activation parameters of the processes. Figure 6 shows the kinetic traces measured at eight temperatures from 5 to 60 °C. The observed kinetics can be adequately described by a double-exponential relaxation at all temperatures. As the temperature is increased, the total change in absorbance decreases, due to a thermal effect on the deligation equilibria of the non-native His residues.

The temperature dependence also evidences the potential of the method we have developed. Kinetics can be followed on submillisecond time scales which allow a wider temperature range to be investigated than is usually possible in conventional mixing experiments.

The activation parameters obtained from a global fitting of the data at all temperatures are reported in Table 1. Similar values could be obtained from the more traditional Arrhenius (illustrated in Figure 7) and Eyring (not shown) plots using single-curve analysis results; these methods gave excellent linear correlations but a less precise estimate of the parameters than the global analysis. The relative weights of the pre-exponential factors, estimated by a global analysis fitting, were constant throughout the temperature range, accounting for 70 ± 7% (His33) and 30 ± 7% (His26) of the overall absorption change. The activation energies, E_a, agree well with literature data, although our estimates of the enthalpic barriers for deligation of His26 and His33 are a bit higher than previously reported (12.3 ± 0.2 kcal/mol for His26 and 17.1 ± 0.7 kcal/mol for His33).[9] The estimates of the activation enthalpies using the Arrhenius (E_a) or the Eyring ($\Delta H^{\ddagger}$) relations[19,31] are fairly consistent and essentially identical at the two GuHCl concentrations used in this work. The activation barriers (E_a, $\Delta S^{\ddagger}$, or $\Delta H^{\ddagger}$) for His33 are systematically larger than the corresponding values for His26, confirming that the axial ligand His33 is the more stable of the two.

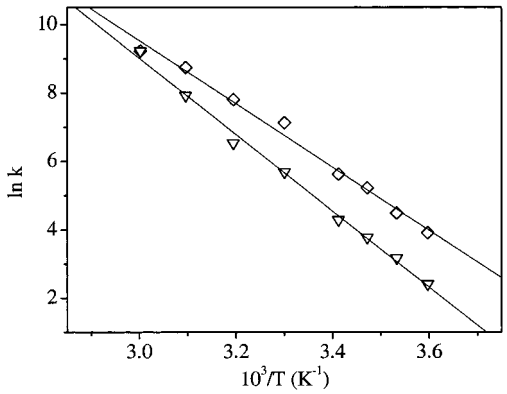

Figure 7. Arrhenius plot for the rate constants $k_1 = 1/\tau_1$ (diamonds, His26), and $k_2 = 1/\tau_2$ (inverted triangles, His33) obtained from the single-curve biexponential fits of the data reported in Figure 6. The parameters obtained from linear analyses of these plots are consistent with the data reported in Table 1, with larger uncertanties.

The larger activation energy for deligation of His33 derives mainly from a higher entropic barrier. Both $\Delta S^{\ddagger}$ values are positive, as observed in many unfolding reactions.[32−34] While $\Delta H^{\ddagger}$ for His33 is only 20% higher than the corresponding value for His26, $\Delta S^{\ddagger}$ is a factor of 2 larger, indicating that deligation of His33 must occur through a transition state with significantly higher entropy than for His26.

Conclusions

We have shown that acid-induced deligation of the non-native histidine ligands from the heme in GuHCl-unfolded Fe(III) cyt *c* can be followed by a laser-induced pH-jump technique with transient absorption detection. Our data nicely reproduce the deligation kinetics previously measured with stopped-flow pH-jump experiments in the millisecond domain. In addition, the superior temporal resolution of the setup allows the investigation of wider temperature ranges in which kinetics fall in the submillisecond range, thereby allowing a better retrieval of activation parameters. The technique promises to be of the greatest help in investigating pH-dependent structural relaxations in protein folding and unfolding studies.

Acknowledgment. C.V. and S.A. acknowledge INFM (sezione B and PRA CADY) for financial support. G. Allodi is kindly acknowledged for providing the Matlab version of Minuit. The work of L.J.L. and E.W.S. was supported by NIH Grant R44 GM51147.

JA010079N

(31) Su, Y. Y. T.; Jirgensons, B. *Arch. Biochem. Biophys.* **1977**, *181*, 137−146.
(32) Scalley, M. L.; Baker, D. *Proc. Natl. Acad. Sci. U.S.A.* **1997**, *94*, 10636−10640.
(33) Su, Z. D.; Arooz, M. T.; Chen, H. M.; Gross, C. J.; Song, T. Y. *Proc. Natl. Acad. Sci. U.S.A.* **1996**, *93*, 2539−2544.
(34) Mohana-Borges, R.; Silva, J. L.; Ruiz-Sanz, J.; DePrat-Gay, G. *Proc. Natl. Acad. Sci. U.S.A.* **1999**, *96*, 7888−7893.